*Research Article*

# Investigation of Wear Behavior of PET Bushings for Turbine Components

Ezgi Özgünerge Falay[1], Öz Erman Arusan[2], Rüçhan Yıldız[3], İsmail Ovalı[4], Engin Tan[5]

[1] ARNES Mechanical Machinery Design Center, Orcid ID: https://orcid.org/0000-0001-6264-2795, E-mail: ezgif@jetseal.com.tr
[2] ARNES Mechanical Machinery Design Center, Orcid ID: https://orcid.org/0000-0002-6312-8533, E-mail: erman@jetseal.com.tr
[3] Department of Metallurgical and Materials Engineering, Pamukkale University, Orcid ID: https://orcid.org/0000-0002-5973-5496, E-mail: ryildiz151@posta.pau.edu.tr
[4] Department of Mechanical Engineering, Pamukkale University, Orcid ID: https://orcid.org/0000-0002-8193-0060, E-mail: iovali@pau.edu.tr
[5] Department of Metallurgical and Materials Engineering, Pamukkale University, Orcid ID: https://orcid.org/0000-0003-4441-3678, E-mail: etan@pau.edu.tr

Received 04 October 2024
Received in revised form 21 December 2024
In final form 24 December 2024

**Reference:** Özgünerge Falay, E., Arusan, Ö. E., Yıldız, R., Ovalı, İ., & Tan, E. (2024). Investigation of wear behavior of PET bushings for turbine components. The European Journal of Research and Development, 4(4), 316-327

## Abstract

*In this study, for the first time, a new generation PET (Polyethylene terephthalate) material bushing design and prototype production by machining was carried out for the turbine blade and adjustment cap blade used in turbine systems within the Arnes Mechanical Machinery Design Center. Within the scope of the study, the tribological properties of the PET material used as the bushing raw material were investigated under different sliding speeds, loads, and sliding distances. Abrasive wear tests were applied using the pin-on-disc method at 3 and 4.5 m/s sliding speeds, 100-, 200-, and 300-meters sliding distances, and 5, 10, 15, and 40 N loads. The wear performance of the PET material was evaluated through the parameters of volume loss, coefficient of friction, and surface roughness. The results obtained showed that the applied load and sliding speed had a significant effect on the wear behavior of the material. The increase in load caused a significant increase in volume loss by creating a higher contact pressure on the material. This situation showed that higher loads create more contact pressure on the surface, causing deformation and material loss in the material's microstructure. It was evaluated that plastic deformation and abrasive wear mechanisms are dominant on the material surface under high loads. In contrast, increasing the sliding speed caused a decrease in the coefficient of friction and surface roughness. It was observed that at higher speeds, the thermal effects caused by friction on the material's surface resulted in the formation of a tribofilm, thus increasing the surface protection capacity of the material and decreasing the coefficient of friction and surface roughness. The findings showed that the bushings manufactured from PET material*

*can be successfully used as an alternative to metal alloy bushings under difficult service conditions in turbine systems.*

**Keywords:** *Turbine Blade, Adjustment Cap Blade, PET Bushing, Wear, Surface Roughness*

## 1. Introduction

Turbine blades and adjustment cap blades are the essential components of turbine systems. These blades direct and control fluids (steam, gas, water, or air) in energy conversion processes. They are functionally designed to ensure turbines' efficient operation and convert fluid energy into mechanical energy. Turbine and regulating gate blades are critical components that complement each other in energy conversion processes. While turbine blades produce mechanical energy, regulating gate blades ensures that this process occurs efficiently and in a controlled manner. Therefore, they have many applications, from power plants to jet engines. Turbine and regulating gate blades are used in steam, gas, and hydraulic turbines [1-3].

The materials to produce these components must be high-strength and resistant to fluid pressure, temperature, and wear. Lightweight materials can increase efficiency by reducing the overall weight of the system. Since turbine and regulating gate blades are exposed to high temperatures and wear, to increase their performance, the bushings used to transfer motion at the connection points and absorb sudden impacts and vibrations must have high mechanical and thermal resistance. PET bushings provide these features while providing an advantage in meeting the need for lightness compared to metal bushings [4-6].

Thanks to the selection of PET materials, the service life of equipment parts is extended, and less frequent replacement is provided. Replacing complex metal parts with PET materials reduces the total weight of the equipment, increases fuel efficiency, and reduces logistics costs. PET materials reduce the risk of corrosion by eliminating metal-to-metal contact and increasing the parts' service life in corrosive environments. With these features, PET materials can be used in areas like the food industry and complex components under high loads, such as pumps, dam gates, hydroelectric power plants, wastewater facilities, cranes, or shipbuilding and offshore areas [7-10].

PET bushings exhibit reliable performance, reduce the wear risk of turbine and adjustment blade covers, and ensure operational continuity. Traditional metal bushings have high production costs. PET bushings, on the other hand, can offer lower-cost production methods. PET bushings can offer superior features by taking advantage of advances in new material sciences. Longer-lasting and more durable PET bushings reduce maintenance and replacement costs, thus reducing total costs [11-13].

This research at the Arnes Mechanical Machinery Design Center led to the development of an innovative PET bushing design and prototype production for use in turbine components. The wear tests and surface roughness measurements applied within the scope of the study provided critical information about the wear performance of PET raw materials. The results showed that the material can be used effectively in engineering applications under difficult service conditions with properties such as superior wear resistance and low coefficient of friction.

PET bushing, developed as an environmentally friendly alternative to metal bushings, significantly contributes to sustainability goals thanks to its recyclability. The low-carbon footprint material used in the production process has allowed for the reduction of environmental impacts and contributed to the development of production processes that align with enterprises' environmental strategies. This innovative approach has provided significant outputs for increasing tribological performance in bushing design processes and has become a valuable solution for engineering and environmental sustainability.

## 2. Materials and Methods

This research includes designing and prototyping a new generation of PET bushings for turbine components such as turbine blades and adjustment valve blades. The properties of the commercial PET material used in the study are given in Table 1.

*Table 1: Properties of PET Material Used in the Study*

| Property | Value | Property | Value |
|---|---|---|---|
| **Density** | 1.35 g/cm$^3$ | **Elongation at Break** | 9.5% |
| **Water Absorption** | 0.30% (23°C) | **Flexural Strength** | 117 MPa |
| **Tensile Strength** | 78 MPa | **Young Modulus** | 2.9 GPa |
| **Yield Strength** | 65 MPa | **Melting Temperature** | 250°C |

The bushing design was carried out within the Arnes Mechanical Machinery Design Center, and its prototype was produced using the machining method. The technical drawing of the designed bushing is given in Figure 1, and the visual of the produced prototype is given in Figure 2.

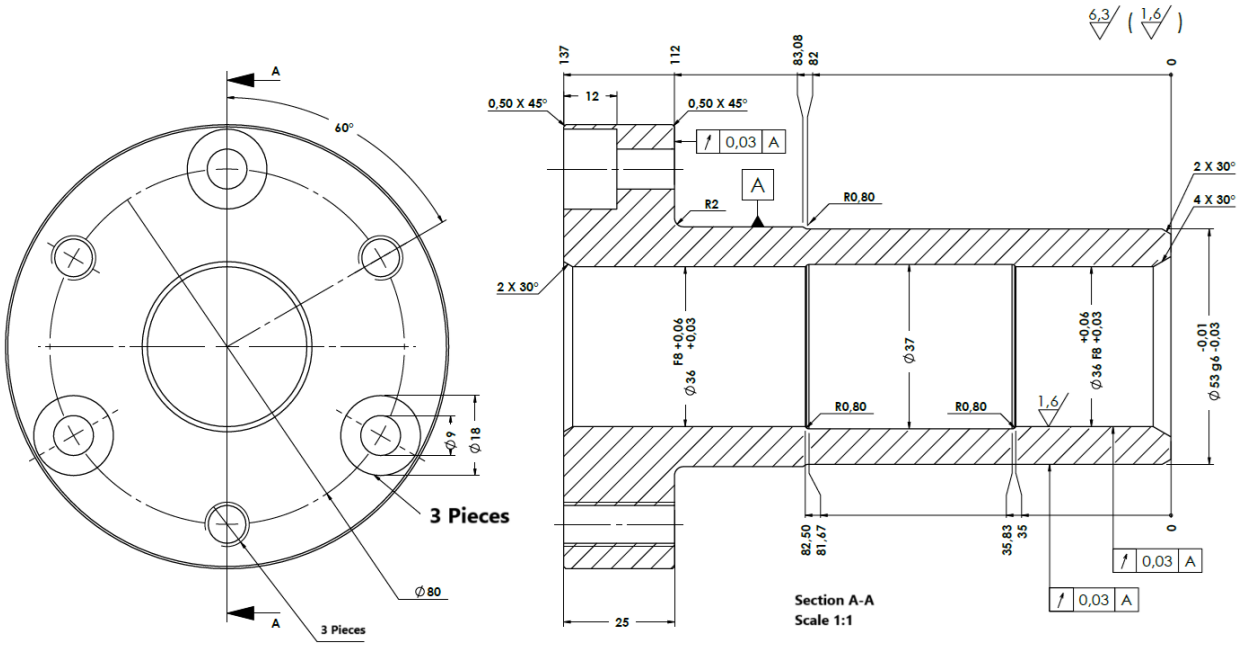


*Figure 1: The Bushing Technical Drawing*

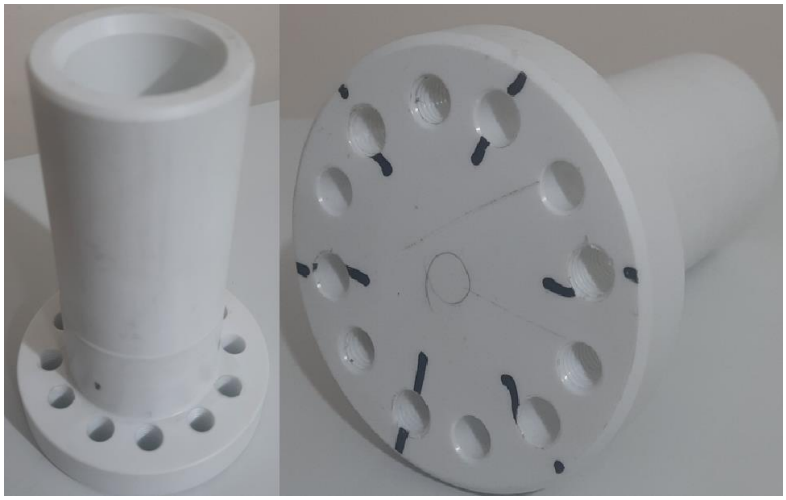

*Figure 2: The Bushing Prototype*

Twenty-four wear test samples were prepared from PET material according to ASTM G99 standards, with the properties given in Table 1. Figure 3 shows the wear test sample dimensions and samples [14].

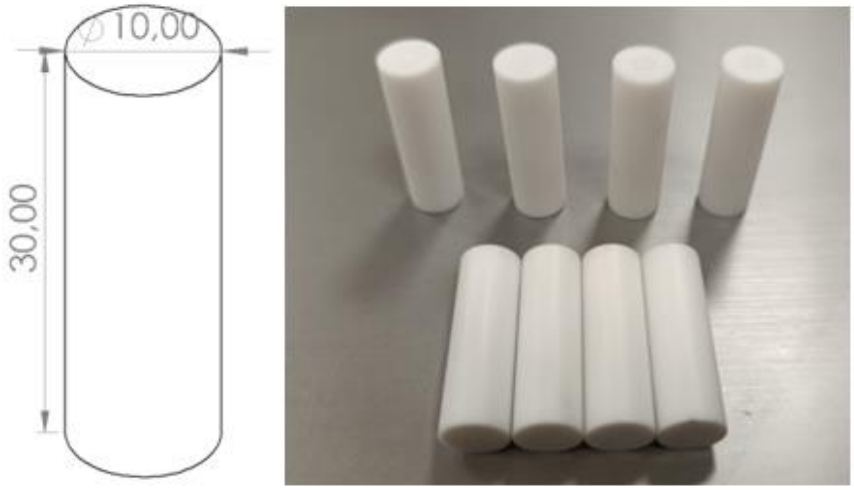


*Figure 3: Wear Test Sample Dimensions and Sample Images*

Before the wear tests, the hardness of the samples was measured on the Shore D scale with the durometer given in Figure 4, and the average hardness value was determined as 84 Shore D.


*Figure 4: Hardness Measurement with Durometer*

The wear test of PET samples prepared in Ø10 x 30 mm dimensions was carried out according to the ASTM G99 standard on the pin-on-disc wear test device given in Figure 5. The wear test was carried out at room temperature without using any lubricant and was performed with 600 mesh SiC sandpaper as abrasive at 3 m/s and 4.5 m/s sliding speeds and 5, 10, 15, and 40 N loads at 100, 200, and 300 m sliding distances.

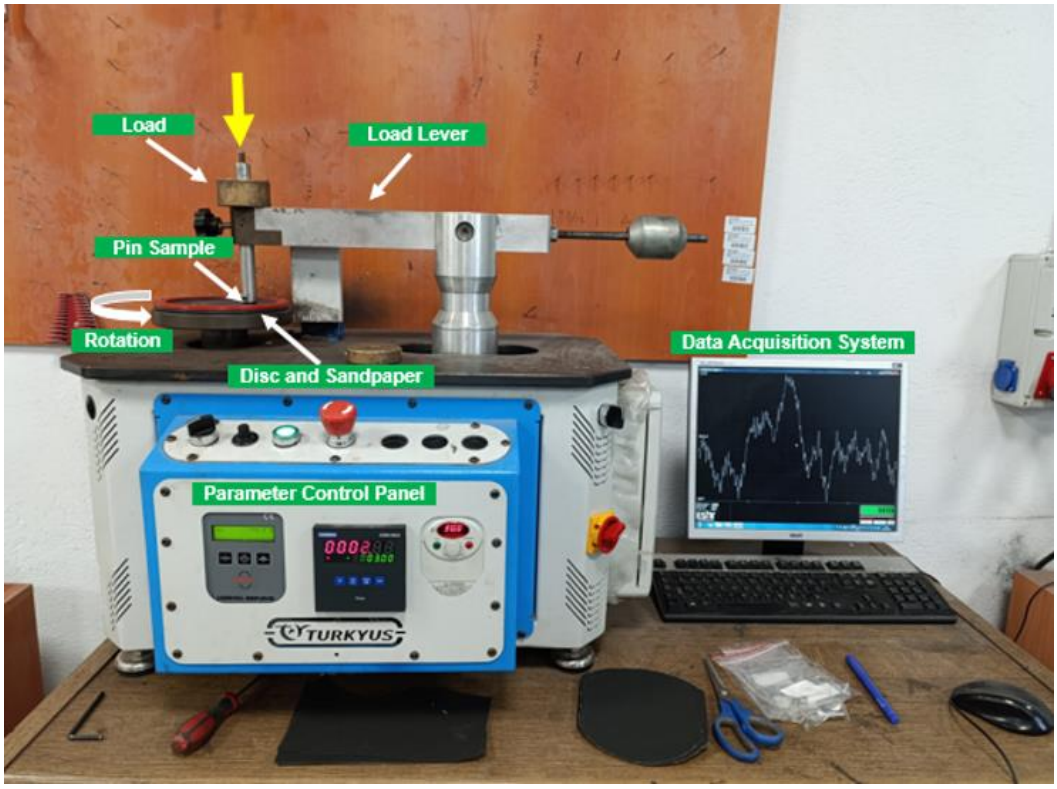


*Figure 5: Pin-on Disc Wear Tester*

Before the test of the samples, their weights were measured with a precision scale, and the initial values were recorded. After the test, the weight measurements were made the same way, and the weight loss was determined. Graphs showing the relationship between volume loss and sliding distance were prepared using the determined weight loss values. In addition, graphs showing the change in the coefficient of friction were drawn using the data obtained from the device's load cell during the test. These graphs were evaluated to understand the material's wear behavior and friction characteristics. The necessary calculations were made according to Equations 2.1. and 2.2. [15].

$$\text{Volume loss } (mm^3) = [\text{Weight loss } (g) / \text{density } (g/cm^3)] \times 1000 \quad (2.1.)$$

$$\text{Coefficient of friction } (\mu) = F/P \quad (2.2.)$$

During the test, the friction force F measured by the load cell in the device represents the friction effect between the sample's surface and the opposite surface. The applied normal load P represents the vertical force applied to the sample during the test.

After the wear tests, surface roughness measurements were performed on the sample, to which a 40 N load and a sliding distance of 300 m were applied. The surface roughness measuring device is shown in Figure 6.

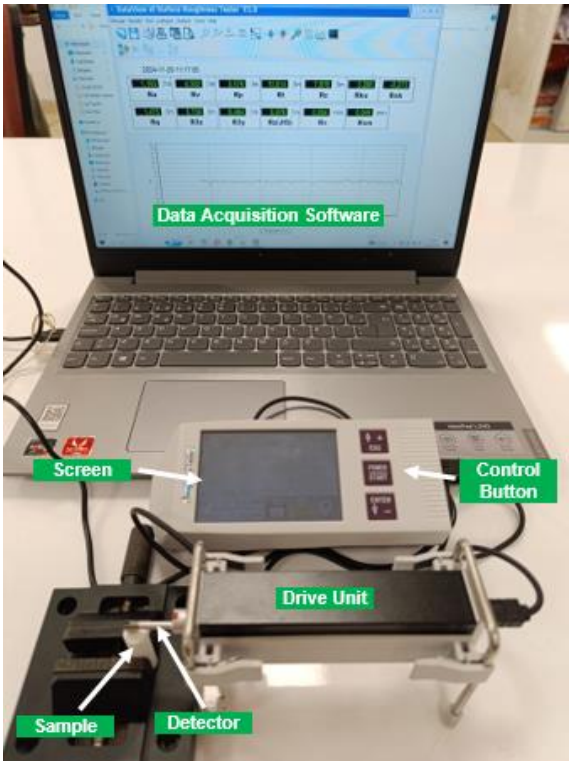


*Figure 6: Surface Roughness Measurement Device*

The wear marks formed on the surface after the wear tests were examined under a Nikon LV 150 NL optical microscope.

## 3. Results

Figure 7 shows the PET material's volume loss ($mm^3$) - sliding distance (m) graph under 3 m/s sliding speed, 5-10-15 and 40 N loads, and 100-200-300 m sliding distance.

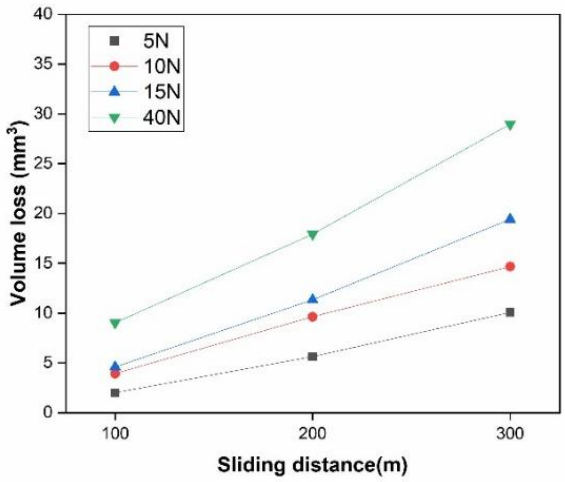


*Figure 7: Volume Loss Depending on the Sliding Distance Under 3 m/s Sliding Velocity*

When Figure 7 is examined, the PET material has lost 10.07 $mm^3$ of volume under a 5 N load, 14.66 $mm^3$ under a 10 N load, 19.40 $mm^3$ under a 15 N load, and 28.96 $mm^3$ under a 40 N at a sliding distance of 300 m. The volume loss increases significantly with increasing load. This is due to increased stress on the contact surface at higher loads. As the load increases, the material surface at the contact points undergoes more plasticity and wears faster. The highest load of 40 N represents where volume loss increases the fastest. Thus, the material surface has reached a critical stress level, and the wear mechanism can be both adhesive and abrasion-related [16].

Figure 8 shows the PET material's volume loss ($mm^3$) - sliding distance (m) graph under 4.5 m/s sliding speed, 5-10-15 and 40 N loads, and 100-200-300 m sliding distance.

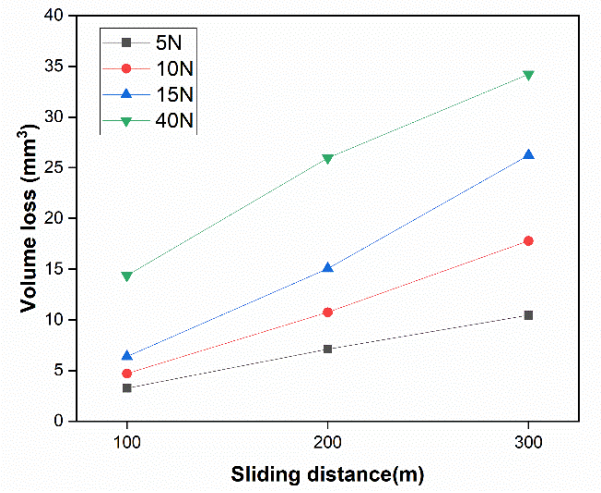


*Figure 8: Volume Loss Depending on the Sliding Distance Under 4.5 m/s Sliding Velocity*

When Figure 8 is examined, it is seen that there is a volume loss of 10.44 $mm^3$ under 5 N load at 300 m sliding distance, 17.77 $mm^3$ under 10 N load at 300 m sliding distance, 26.22 $mm^3$ under 15 N load at 300 m sliding distance, 34.22 $mm^3$ under 40 N at 300 m sliding distance. Volume loss generally increased significantly with the increase in sliding speed. It clearly shows that sliding speed, load, and sliding distance directly affect wear behavior. In evaluating wear behavior, volume loss is one of the most important parameters in understanding the material's resistance to wear. The analyses revealed that volume loss increases significantly with the increase in sliding speed. This increase becomes more pronounced mainly due to changing load and sliding distances. This increase in volume loss with the increase in sliding speed is generally due to increased deformation on the material surface. At higher sliding speeds, the temperature increase caused by friction causes the material to soften, making it more vulnerable to wear. An increase in the sliding distance means an increase in the contact time. This allows wear mechanisms (e.g., adhesion, abrasion, or surface fatigue) to act longer, resulting in more wear on the material surface. These findings emphasize the importance of considering

factors such as sliding speed, load, and distance in the design of wear-resistant materials [17].

Figure 9 gives the coefficient of friction graph depending on the sliding distance under sliding speeds of 3 m/s and 4.5 m/s.

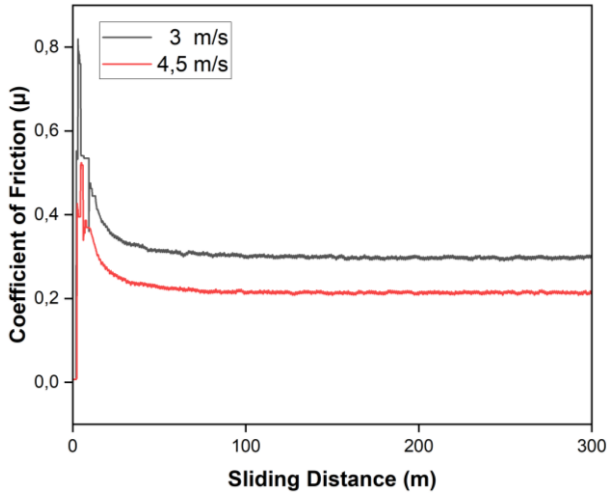


*Figure 9: The Coefficient of Friction Depending on the Sliding Distance Under Sliding Speeds of 3 m/s and 4.5 m/s*

The highest coefficient of friction was obtained at 3 m/s (approximately 0.316-342 μ), while the lowest was obtained at 4.5 m/s sliding speed (0.208-0.238 μ). The decrease in the coefficient of friction under the speed of 4.5 m/s can be explained as the material's surface being flattened due to exposure to more thermal effects. When Figure 9 is examined, it is understood that the changes occurring during wear cause the force acting on the material to vary; therefore, fluctuations are observed. These fluctuations are associated with the force changes that the material is exposed to during events such as boiling and rupture. A sudden decrease in the coefficient of friction was observed at both speeds. This shows that the surfaces did not adapt to each other at the beginning and that there was intense micro-wear and material transfer in the initial contact area. The sudden changes in the coefficient of friction are remarkable due to the surfaces trying to adapt during the initial contact. As the sliding distance increases, the coefficient of friction becomes more stable [18].

One of the important parameters in the examination of wear characteristics is surface roughness. After the wear experiments, surface roughness measurements of the friction surfaces were performed. Surface roughness measurements were performed on the surface to which a 40 N load was applied and on the wear marks after a sliding distance of 3000 m. The surface roughness measurement results at 3 m/s and 4.5 m/s sliding speeds

are given in Figure 10. It was determined that the surface roughness decreased with increasing sliding speed. While the Ra value was 1.558 at a sliding speed of 3 m/s, it became 1.162 when the sliding speed increased to 4.5 m/s. The sliding forces formed at high speeds erode the micro-ridges (roughness) on the surface and create a smoother contact surface. This reduces friction by making the surface contact more homogeneous. A local softening due to heating may occur on the surface at high sliding speeds, especially in polymers. This facilitates the deformation of micro-ridges (roughness) and causes the surfaces to become smoother. As a result, the surface roughness Ra value decreases at certain speed levels [19].

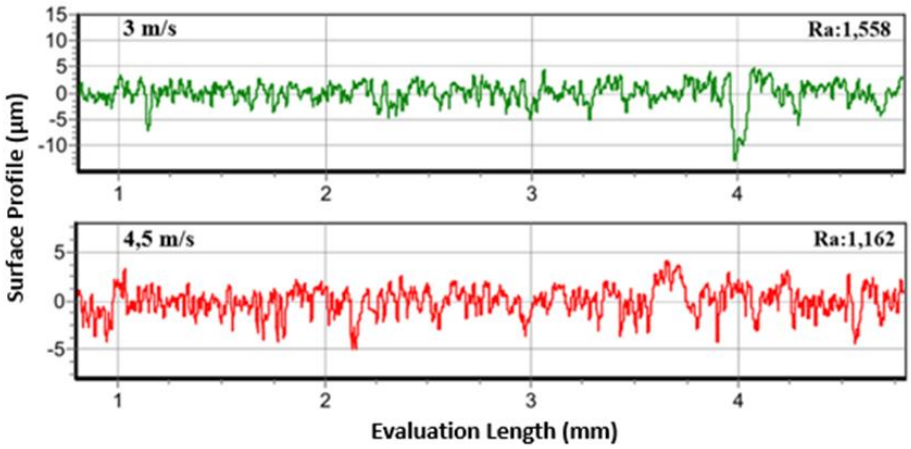


*Figure 10: Surface Roughness Measurement Results at 3 m/s and 4.5 m/s Sliding Speeds*

Figure 11 shows the image of the wear marks formed on the surface after wear. As can be seen, the surface roughness is high at a speed of 3 m/s, and the wear marks appear more profound and more prominent. The wear marks are shallower at a speed of 4.5 m/s, and the surface roughness is low. Increasing roughness on the contact surface causes a decrease in the contact area. Thus, the decrease in the contact area due to increased wear debris and surface roughness is attributed to the decrease in friction [20].

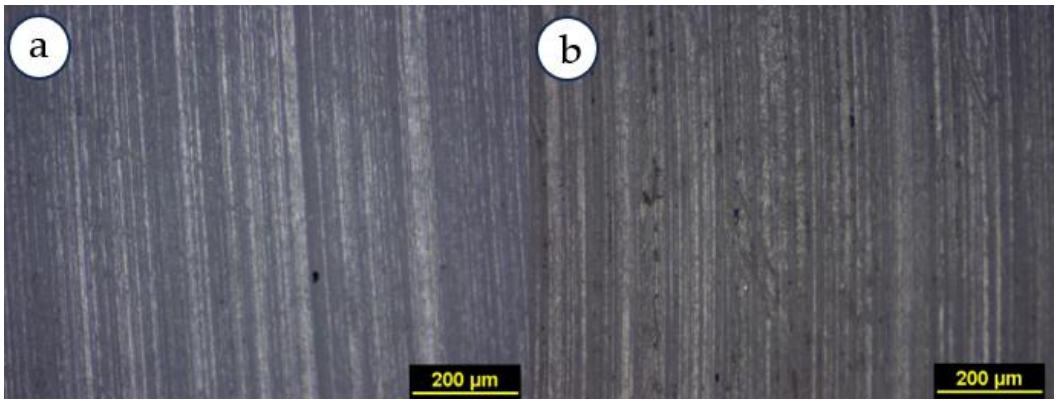


*Figure 11: Surface Wear Traces at Sliding Speeds of a. 3 m/s and b. 4.5 m/s*

## 4. Discussion and Conclusion

This study determined the abrasive wear performance of the new generation PET bushing designed and prototyped for use in turbine blades and adjustment cap blades. The general results of the study are given below:

- In wear, due to increased stress and plasticity on the contact surface at higher loads with increasing load, volume loss increased significantly. Adhesive and abrasive wear acted together at maximum load.
- The increase in sliding speed resulted in effective volume loss. Changing load and sliding distances made the effect of this increase more apparent. The increase in deformation on the material surface directly affected the volume loss. Therefore, the importance of parameters such as sliding speed, load, and distance in wear-oriented material design has been shown.
- The coefficient of friction decreased with increasing sliding speed. Flattening on the surface due to thermal effects explains this result. The decrease in the coefficient of friction showed intense microwear and material transfer in the initial contact area. The coefficient of friction became stable as the sliding distance increased.
- Surface roughness decreased with increasing sliding speed. Increasing sliding forces at high speeds reduced the micro peaks on the surface, resulting in a smoother contact surface. Thus, friction decreased.
- Increasing sliding speeds resulted in shallower wear marks. This finding can be associated with low surface roughness.
- It is suggested that examining the parameters (such as machinability and tool wear) for machining in the production of new-generation PET bushings in subsequent studies will positively contribute to material performance, cost-effectiveness, and environmental impacts.

## References

[1] Villagran, Y., Gomez, L. H. H., Ortiz, M. P. & Beltrán-Fernández, J. A. (2019). Analysis of the wear damage on offshore gas turbine blades. In book: Engineering Design Applications, 221-236.

[2] Schlobohm, J., Bruchwald, O., Frackowiak, W. & Li, Y. (2016). Turbine blade wear and damage – An overview of advanced characterization techniques. Materials Testing, 58(5), 389-394.

[3] Chen, H., Pan, J., Wang, S., Ma, J. & Zhang, W. (2024). Fatigue damage assessment of turbine runner blades considering sediment wear. Applied Sciences, 14(11), 4660.

[4] Czerniec, M., Czerniec, J. & Zubrzycki, J. (2024). Mathematical modeling of load capacity and durability of metal-polymeric bearings with a composite bushing based on polyamides, polytetrafluoroethylenes, polyetheretherketones, or polyethylene terephthalates. Applied Sciences, 14(23), 11275.

[5] Antwi-Afari, M. F., Mi, H. Y. & Liu, C. (2023). Research on the feasibility of polyethylene terephthalate foam used in wind turbine blades. Enviromental Progress & Sustainable Energy, 42(1), e13956.

[6] Walczak, M. & Caban, J. (2021). Tribological characteristics of polymer materials used for slide bearings. Open Engineering, 11(1), 624-629.

[7] Guan, M., Jin, H., Wei, W. & Yan, M. (2023). Degradation of polyethylene terephthalate (PET) and polypropylene (PP) plastics in seawater. DeCarbon, 1, 100006.

[8] Goujon, N., Demarteau, J., Lopez de Pariza, X., Casado, N., Sardon, H. & Mecerreyes, D. (2021). Chemical upcycling of PET waste towards terephthalate redox nanoparticles for energy storage. Sustainable Chemistry, 2(4), 610-621.

[9] Duan, C., Wang, Z., Zhou, B. & Yao, X. (2024). Global polyethylene terephthalate (PET) plastic supply chain resource metabolism efficiency and carbon emissions co-reduction strategies. Sustainability, 16(10), 3926.

[10] Sarda, P., Hanan, J. C., Lawrence, J. G. & Allahkarami, M. (2021). Sustainability performance of polyethylene terephthalate, clarifying challenges and opportunities. Journal of Polymer Science, 60(1), 7-31.

[11] Zhang, J., Darwish, N., Coote, M. L. & Ciampi, S. (2020). Static electrification of plastics under friction: The position of engineering-grade polyethylene terephthalate in the triboelectric series. Advanced Engineering Materials, 22 (3), 1901201.

[12] Gutnikov, V.A., Kaykazsky V. I. & Usanova K.I. (2024). High performance polymer Zedex-100K based on polyethylene terephthalate: physical, mechanical and operational properties. AlfaBuild, 30, 3005.

[13] Domitran, Z., Zezelj, D. & Katana, B. (2016). Influence of contact pressure and sliding speed on the temperature and coefficient of friction in sliding contact between two PET samples. Tehnički Vjesnik 23(2), 389-396.

[14] ASTM G99-17. (2017). Standard test method for wear testing with a pin-on-disk apparatus, ASTM International, West Conshohocken, PA.

[15] Ovalı, İ. (2017). Abrasive wear behavior of various reinforced AA6061 matrix composites produced with hot pressing process: A comparative study. Materialwissenschaft und Werkstofftechnik, 48(6), 589–599.

[16] Sukumaran, J., De Pauw, J., Neis, P. D., Tóth, L. F. & De Baets, P. (2017). Revisiting polymer tribology for heavy duty application. Wear, 376-377, Part B, 1321-1332.

[17] Tóth, L. F., Sukumaran, J., Szebényi, G. & De Baets, P. (2019). Tribo-mechanical interpretation for advanced thermoplastics and the effects of wear-induced crystallization. Wear, 440-441, 203083.

[18] Cho, D. H., Bhushan, B. & Dyess, J. (2016). Mechanisms of static and kinetic friction of polypropylene, polyethylene terephthalate, and high-density polyethylene pairs during sliding. Tribology International, 94, 165-175.

[19] Bhushan, B., & Ko, P. L. (2003). Introduction to tribology. Applied Mechanics Reviews, 56(1), B6-B7.

[20] Myshkin, N. K., Petrokovets, M. I., & Kovalev, A. V. (2005). Tribology of polymers: Adhesion, friction, wear, and mass-transfer. Tribology International, 38(11-12), 910-921.